

BASIC STUDY ON THE REAL-TIME THREE-DIMENSIONAL POSITION MEASUREMENT OF GROUND MOVING OBJECTS USING AN ACCELEROMETER AND GYROS

Yoshiwo OKAMOTO*, Toshio KOIZUMI**, Yasuyuki SIRAI***

*Dep. Electrical, Electronics and Computer engineering, Professor, Chiba Institute of Technology,
2-17-1, Tsudanuma, Narashino-shi, Chiba 275-0016, Japan - okamoto@ec.it-chiba.ac.jp

**Dep. Architecture and Civil Eng., Professor, Chiba Institute of Technology,
2-17-1, Tsudanuma, Narashino-shi, Chiba 275-0016, Japan - koizumi@pf.it-chiba.ac.jp

***Dep. Design, Associate Professor, Chiba Institute of Technology,
2-17-1, Tsudanuma, Narashino-shi, Chiba 275-0016, Japan - shirai@pf.it-chiba.ac.jp

Commission I, WG I/2

Keywords: Surveying, Development, Measurement, Navigation, Platforms, Mobile, Three-dimensional

ABSTRACT

In recent years, electronics and computer technology have been applied to the development of survey instruments, and the methods of measurement have widely changed. We make use of sophisticated systems in daily base such as Total-Station, GPS and Laser-scanner, to name a few. However, a system based on light wave and/or radio wave has a weakness that it would not work if the waves were intercepted. An inertial survey system, on the other hand, functions independently of those waves, and it must be convenient under such circumstances. Therefore the authors are developing a portable and low-priced strap-down inertial navigation system. In this paper, the results from the field tests are presented, which have been performed on the equipment made on an experimental basis in order to investigate how the accuracy depends on the measurement strategy, namely the nonstop or the stop-and-go strategy.

1 INTRODUCTION

For mobile mapping and various other purposes, it is an important research subject to measure accurately the three-dimensional position of a platform on real-time basis. GPS has been commonly used for these purposes. However, GPS sometimes does not work in urban areas with a number of towering buildings and/or mountainous rural areas because of the electromagnetic interference or blockage. By making use of the technique known as "inertial survey", the authors had developed a system capable of measuring three-dimensional position of a ground-moving object on a real-time basis using accelerometers and gyros even in an area where GPS does not work. In the inertial survey system, positions are determined by integrating accelerations and angular velocities obtained from sensors. Therefore, the accuracy decreases as the measuring time becomes longer because of the accumulation of errors. In order to overcome these difficulties, the authors propose a modified method in which stop-and-go procedures are repeated during one sequence of measurement, and the integrated value of acceleration (velocity) is forced to be zero at every stoppage by subtracting linear drift so that errors do not

accumulate any more. They also performed experimental measurements so as to evaluate the effectiveness of this method. Their results are shown in this paper.

In this study, servo-type accelerometers and two types of gyros were used: one is the vibration gyro that is inexpensive but has somewhat lower performance, and the other is the fiber optical gyro with moderate performance. By attaching an accelerometer and a gyro to each of three mutually orthogonal axes, a strap-down inertial survey system was constructed. As a platform, a bicycle trailer was used. Experiments were performed on an asphalt-paved road with horizontal distance of about 160 meters and level difference of about 6 meters. Resultant time courses of the platform location were compared with the actual ones in both the horizontal plane and vertical alignments of the road. Two kinds of measurement strategy were tested: the conventional one in which the equipment moves without any stoppage and the one with repeated stop-and-go, which had been proposed by the authors. They shall be called the nonstop strategy and the stop-and-go strategy, respectively, hereafter in this paper.

2 EQUIPMENT USED IN THE PRESENT STUDY

As mentioned in the previous section, servo-type accelerometers and two types of gyros were used in the present study. Their specifications are listed in table 1 through table 3. As shown in figure 1, a strap-down inertial navigation system was constructed by attaching an accelerometer and a gyro to each of three mutually orthogonal axes. Figure 2 shows the equipment made on an experimental basis, which was used in the present study.

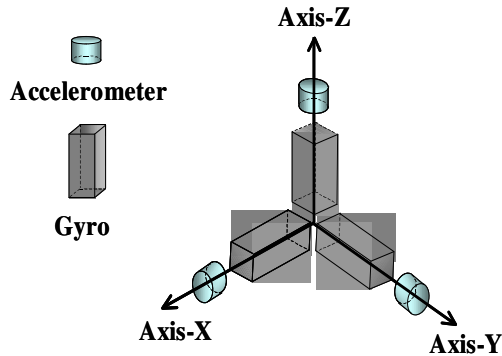


Figure 1. Coordinate system and sensors

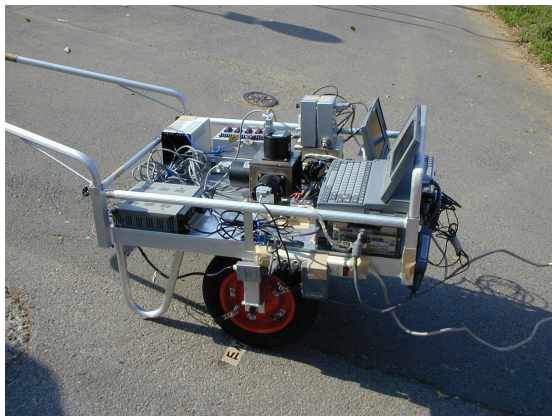


Figure 2. Experimental equipment

3 MEASUREMENT STRATEGY SUITABLE FOR INERTIAL SURVEY

3.1 Route alignment

Experiments were performed on the asphalt-paved road with about 5.5 m elevation difference and 164 m inclined length. Alignment of the road was measured in detail using a total station and a digital level, and the result was considered as the true alignment in the following experiments concerned with our inertial survey system. Figure 3 and 4 show the plane and the vertical alignment, respectively, used in the experiments.

Table 1. Specification of accelerometer JA-5V

Item	Specification	
Resolution	$< 1 \times 10^{-4}$ (with LP filter)	
Sensitivity	$5V/G \pm 3\%$	
Zero point unbalance	$< \pm 0.01\%$	
Largest measuring range	$\pm 2G$	
Lateral sensitivity	$< 0.01\%$	
Power sup.	Voltage	$\pm 12 \sim \pm 18V$ DC
	Current	$< 20mA$
Weight	$< 80gf$	

Table 2. Specification of Vibration gyro ENV-05A

Item	Specification	
Resolution	$0.1^\circ/s$	
Detection range	$\pm 90^\circ/s$	
Responsibility	DC ~ 7Hz	
Power sup.	Voltage	$+8 \sim +13.5V$ DC
	Current	$< 15mA$
Weight	$< 45gf$	

Table 3. Specification of fiber optical gyro JG-35FD

Item	Specification	
Resolution	$0.06^\circ/s$	
Detection range	$\pm 90^\circ/s$	
Responsibility	DC ~ 20Hz	
Power sup.	Voltage	12V DC
	Current	$< 1A$

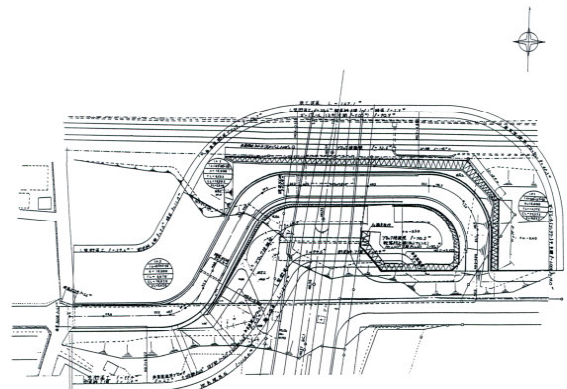


Figure 3. Plan of experiment place

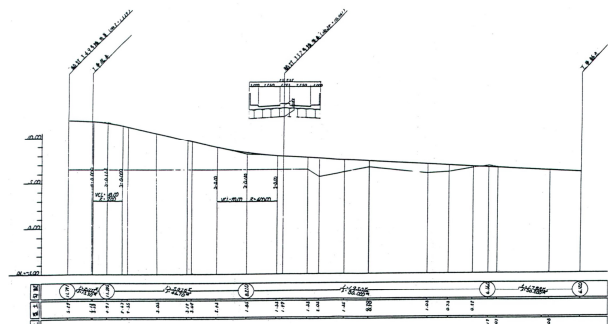


Figure 4. Running through chart

3.2 Fixed and moving coordinate systems

Two kinds of coordinate system are used in the experiments: the one denoted by $\Sigma(XYZ)$ is fixed to the ground such that X - Y plane is horizontal and X -axis directs toward magnetic north, and the other one denoted by $\Sigma(xyz)$ moves with the equipment. They shall be called the fixed coordinate system and the moving coordinate system, respectively. Both systems coincide with each other at the beginning of the experiment, but the system $\Sigma(xyz)$ translates and rotates as the inertial navigation system goes along the route. Accelerations and angular velocities obtained from the sensors are the vector components in the moving coordinate system $\Sigma(xyz)$. Therefore, they are transformed into those in the fixed coordinate system $\Sigma(XYZ)$ before integration, and the rest of the computations (e.g. positioning and error evaluation) are performed in $\Sigma(XYZ)$.

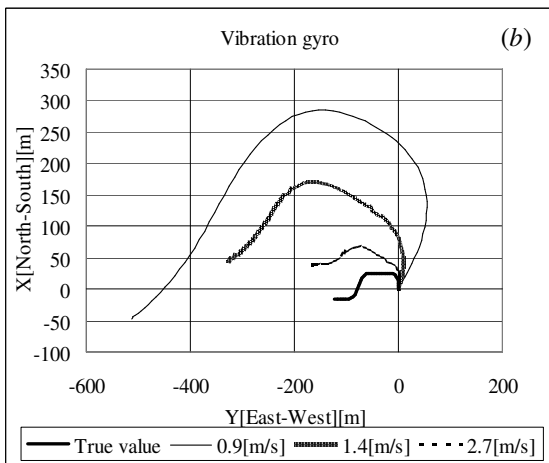
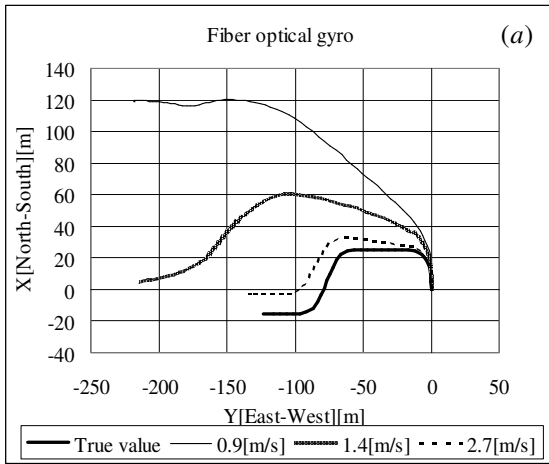


Figure 5. Estimated trajectories projected onto a horizontal plane (nonstop strategy)

3.3 Effects of the moving speed

In inertial survey, the distance is obtained by integrating the acceleration twice, and the angular change is obtained by integrating the angular velocity once. The error accumulates and increases with the lapse of time, and hence it seems desirable to finish the measurement in shorter time to make the positioning more accurate. In order to ascertain whether this inference is correct or not, experiments were repeated changing the moving speed of the equipment. The nonstop strategy is adopted in this experiment with three kinds of moving speed: slow (approximately 3 min. to go around whole the route, approximately 0.9 m/s), medium (2 min., 1.4 m/s) and fast (1 min., 2.7 m/s).

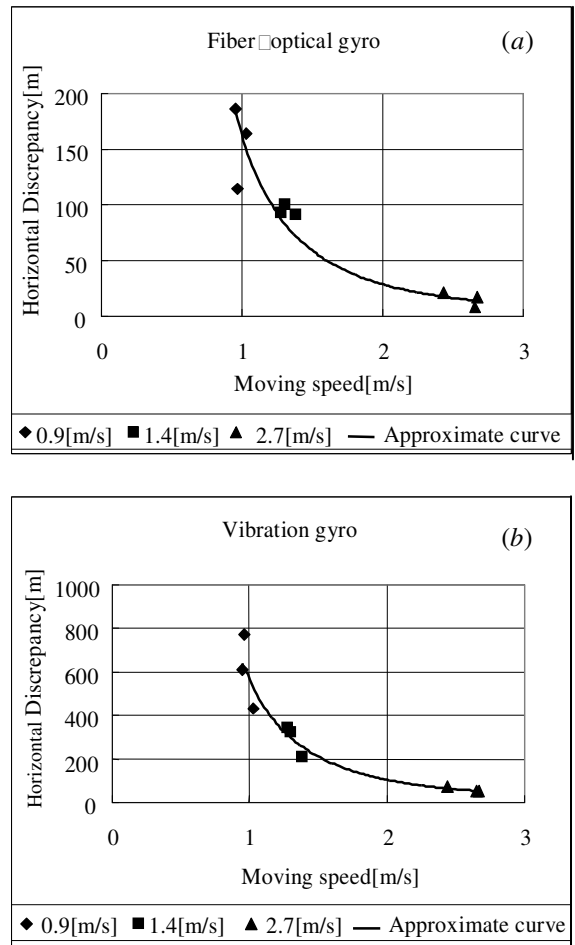


Figure 6. Dependence of the horizontal discrepancy on the moving speed (nonstop strategy)

Figure 5(a) shows the estimated trajectories by the inertial navigation system equipped with fiber optical gyros. They are projected onto a horizontal plane. Thick solid curve represents the true trajectory mentioned in section 3.1, and other three curves stand for the estimated trajectories in cases that the moving speed is slow, medium and fast, respectively. As has been expected, the discrepancy between the true and the estimated trajectories decreases as the moving speed increases. If

the fiber optical gyros are replaced with the vibration gyros, we get the results shown in figure 5(b). Since the resolution of the vibration gyro is lower than that of the fiber optical gyro, the discrepancy is larger in figure 5(b) than that in 5(a). In order to evaluate the discrepancy quantitatively, “the horizontal discrepancy ε_h ” is defined as the horizontal distance between the true position and the estimated one at the end point of the route, namely $\varepsilon_h = ((X_e - X_t)^2 + (Y_e - Y_t)^2)^{1/2}$ where the subscripts “e” and “t” refer to the estimated and the true coordinates of the end point, respectively. The dependence of the horizontal discrepancy on the moving speed is plotted in figure 6. The experiments were repeated three times for each moving speed, and hence three points are plotted for each moving speed in both panels of figure 6.

3.4 Effects of the stop-and-go strategy

The stop-and-go strategy was proposed in order to suppress accumulation of integration errors due to random drift of the accelerometers and gyros. In this strategy, the equipment moves from the starting point \mathbf{R}_0 and halts at a point \mathbf{R}_1 on the route, then it moves from \mathbf{R}_1 and halts at the next point \mathbf{R}_2 on the route, and so on. These procedures are repeated until the equipment reaches the end point \mathbf{R}_N . Suppose that the equipment leaves from \mathbf{R}_{n-1} at time point t_n and gets to \mathbf{R}_n at T_n , which means that the equipment moves during the time interval $[t_n, T_n]$ for $n=1 \sim N$ and stays still during $[T_n, t_{n+1}]$ for $n=1 \sim N-1$. Suppose more that the integration of the acceleration $\mathbf{a}(t)$ measured by the accelerometers over the interval $[t_n, T_n]$ is \mathbf{v}_n , which would be $\mathbf{0}$ if the measured acceleration were free from noise. Then, in order to make the velocity at T_n zero, $\mathbf{a}(t)$ is replaced with $\mathbf{a}(t) - \mathbf{v}_n / (T_n - t_n)$ in the interval $[t_n, T_n]$. This method of compensation is known as ZUPT (Zero-velocity Up Dates). Anyway, in order to make this method effective, it is crucial to record the timings t_n, T_n accurately.

In the actual experiment performed this time, the stopping points \mathbf{R}_n ($n=0 \sim N$) are arranged uniformly over the route with the distance between the adjacent points, or the stoppage interval, about 3, 5, 10, 20, 30, and 50m. This means that the experiment was repeated 6 times with these 6 choices of stoppage interval. The velocity of the equipment was kept as constant as possible to about 1.4 m/s that is referred as “medium speed” in the previous section, and the length of the time interval $[T_n, t_{n+1}]$ or the stay time is chosen to be 5s. In each panel of figure 7, the true trajectory is plotted with a thick solid line as the same in figure 5, while a thin solid curve represents the estimated one by means of the stop-and-go strategy in the case that the stoppage interval is 10m. Moreover, the estimated trajectory by means of the nonstop strategy with medium moving speed is also plotted with a thin dotted line as a comparison. It is clear that the estimation error is reduced drastically by means of the stop-and-go strategy.

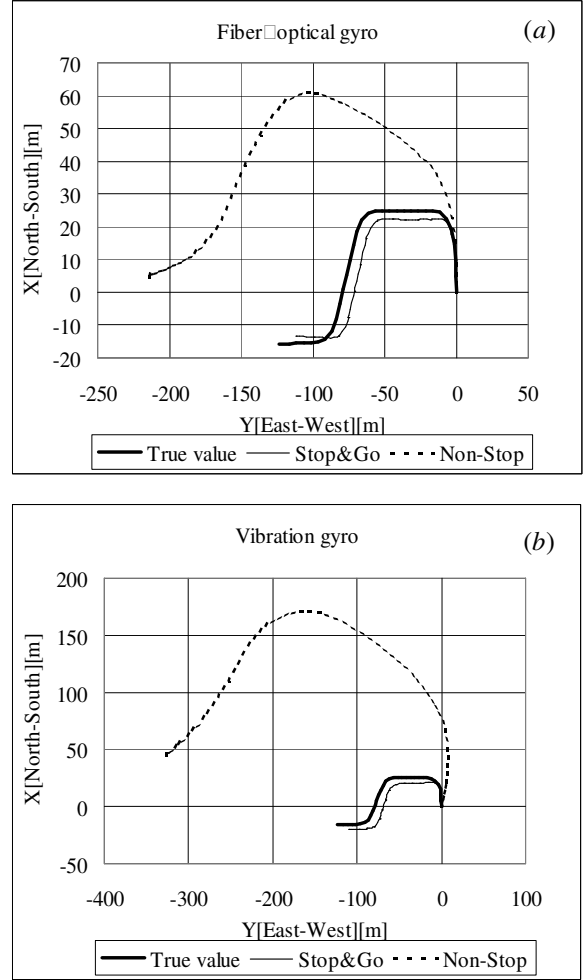


Figure 7. Trajectories estimated by means of stop-and-go and nonstop strategies

4 BIAS CORRECTION

When the accelerometers and gyros stay still, their outputs should be zero. However, in reality, some nonzero output called the bias error is observed even from a sensor at a standstill as described in figure 8. The bias error α_B in the acceleration yields the positioning error $\alpha_B t^2 / 2$ where t is the elapsed time, while the bias error ω_B in the angular velocity causes the angle error $\omega_B t$. The magnitudes of bias errors observed from the sensors used in the present experiments are listed in table 4. The positioning and angle errors due to these bias errors are plotted in figure 9 as functions of the elapsed time. As can be seen in this figure, the positioning errors become 16, 70 and 6m along X, Y and Z axes, respectively, when the elapsed time is 60s. In the case of fiber optical gyros, the angle errors 60s after the onset are 3.2, 1.1 and 0.3 degrees around X, Y and Z axes, respectively, while they are as large as 47, 38 and 5 degrees in the case of vibration gyros.



Figure 8. Bias error

Table 4. Bias errors contained in the sensors

Item	X-axis	Y-axis	Z-axis
Accelerometer [m/s^2]	0.005	0.020	-0.002
Fiber optical gyro [$^\circ/\text{s}$]	0.053	0.018	0.004
Vibration gyro [$^\circ/\text{s}$]	0.788	0.639	0.082

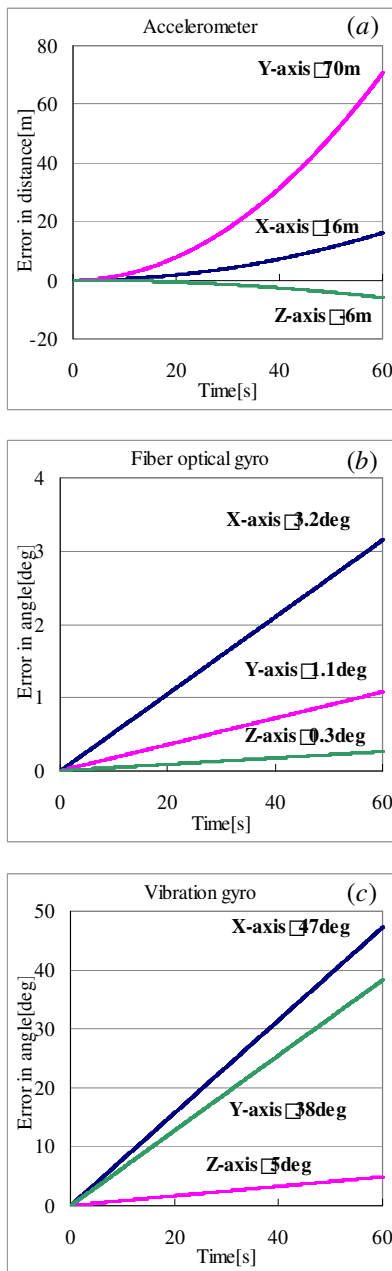


Figure 9. Positioning and angle error due to bias error

The bias errors are estimated at each stopping point \mathbf{R}_{n-1} ($n=1 \sim N$) as the averages of 50 consecutive outputs from the sensors sampled at every 2ms during the time interval $[t_n - 1, t_n]$. As mentioned before, the equipment leaves from \mathbf{R}_{n-1} at time point t_n , so the averages are taken over the one-second intervals just before leaving times. Then, the bias errors thus estimated are subtracted from the measured values of accelerations and angular velocities during the time interval $[t_n, T_n]$ so as to eliminate their effects. This method of bias elimination should be called “the bias correction”. In figure 10(a) shows the trajectories projected on a horizontal plane estimated by means of the stop-and-go strategy with and without the bias correction in the case that the stoppage interval is 10m. In figure 10(b), the elevations or z-coordinates are plotted as functions of the horizontal distance that is defined as the length from the starting point along the route projected on a horizontal plane. As can be seen from this figure, the discrepancy between the estimated trajectory and the true one is notably reduced by correcting the bias errors.

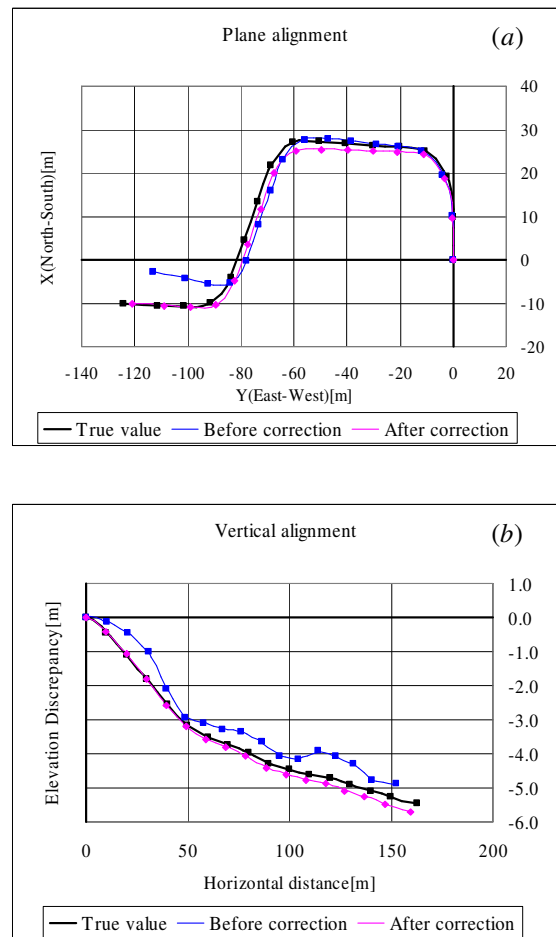


Figure 10. Effects of the bias correction applied to the inertial survey together with the stop-and-go strategy.

5 CONCLUSIONS

Conclusions are as follows:

- (1) The stop-and-go strategy proposed by the authors makes the inertial survey more accurate than the conventional nonstop strategy.
- (2) The accuracy increases as the speed of the equipment increases.
- (3) The accuracy is strongly influenced by the performance of gyros.
- (4) The accuracy is improved by the stop-and-go strategy even with low-performance gyros.
- (5) The bias correction is quite effective, especially when it is used together with the stop-and-go strategy, to improve the accuracy.

REFERENCES

- 1) Innes J.: Inertial platform techniques for rapid surveys of hilliness and bendiness, *Sensors Highway and Civil Engineering*; London, p.143-154, 1981
- 2) Chapman W. H.: Proposed specifications for inertial surveying, *Tech. Paper Annu. Meeting American Congr. Survey Mapping*, No.43, p.287-293, 1983
- 3) Roof E. F.: Inertial survey systems, *J. Surv. Eng* □ Vol.109, No.2, p.116-135, 1983
- 4) Cross P. A.: Inertial surveying, *Int. J. Remote Sensing*, Vol.6, No.10, p.1585-1589, 1985
- 5) Suzuki H. et al.: Real-time measurement of altitude data using the accelerometer, *International Archives of Photogrammetry and Remote Sensing*, Hakodate, Vol. XXXII, Part 5, p.278-283, 1998
- 6) Koizumi T. et al.: Fundamental study on development and application of the local positioning system using accelerometer and gyroscope, *Proc. Int. Workshop on Mobile Mapping Technology*, Bangkok 6B-5-1 - 6B-5-6, 1999
- 7) Shirai Y. et al.: Fundamental study on real time measurement of altitude data with accelerometer and vehicle speed sensor, *International Archives of Photogrammetry and Remote Sensing*, Amsterdam, Vol. XXXIII, Part B1, p.301-306, 2000